



## Passive proliferation of convective heat transfer consummated with nanoporous surface

S. Kalaiselvam\*, M.S. Gugan, E. Kuraloviyar, R. Meganathan, A. Niruthiya Priyan, M.R. Swaminathan

Refrigeration and Air Conditioning Division, Department of Mechanical Engineering, Anna University, Chennai, India

### ARTICLE INFO

#### Article history:

Received 11 May 2009

Received in revised form

23 October 2009

Accepted 26 October 2009

Available online 25 November 2009

#### Keywords:

Convective heat transfer

Electrochemical anodization

Spray pyrolysis

### ABSTRACT

This paper analyses the passive augmentation of convective heat transfer administering the nanoporous layers fabricated by electrochemical anodization and spray pyrolysis. Nanoporous structures fabricated in electrochemical anodization have pore size varying from 40 to 120 nm, and the pore size procured in spray pyrolysis fluctuates from 60 to 100 nm. Convective energy transfer greatly banks on surface attributes. These nanoporous structures aid in hindering the dynamic flow of fluid and the turbulence is achieved more expeditiously. The proliferation of the convective heat transfer obtained with electrochemically anodized nanoporous surface is 131% higher than the polished bare metals with surface roughness 0.2  $\mu\text{m}$ . In case of spray pyrolysis the maximum proliferation is 120%. Disparate disciplines of nanoporous fabrication are perused for asserting a productive process. This paper also analyses the control parameters in the nanoporous fabrication process.

© 2009 Elsevier Masson SAS. All rights reserved.

### 1. Introduction

Heat transfer enhancement is the denouement to encounter the future energy expectations in economic energy management. Heat transfer can be ameliorated by active and passive techniques. Active techniques subsume electric energy to initiate turbulence. Acoustic fields or swirl generators are used to produce surface vibrations. Active approaches are so esoteric and expensive to implement in commercial production. Passive techniques mainly utilize idiosyncrasies of flow velocity and surface roughness. Fins, fluid additives and surface roughness are also employed to augment the heat transfer. Passive techniques are more beneficial than active method accounting for the containment of greenhouse gases to pave way for a greener environment. The sphere of passive heat transfer enhancement technology has been stoked up by the recent developments in the field of nano technology. Exploiting the nanoporous structures to escalate the heat transfer rate is preponderant proposal for efficient energy management. Surface geometry, flow velocity, flow turbulence are the influential ingredients on which heat transfer attributes rely on.

Swirl generators are employed to produce the flow turbulence for increased heat transfer. The augmentation of heat transfer achieved is 20% and it is a function of momentum ratio and Reynolds number [1]. Flow on undulated wavy surfaces with grooves and fins contribute to the higher thermal efficiency [2,3]. Another passive procedure to enhance the heat transfer is by decimating the pipe diameter. It boosts the flow velocity aiding the convective medium to transport more heat energy from the surface. Shrinking the pipe diameter beyond the critical limit of 0.20 mm boosts the flow velocity building up the pressure losses in the system. This system will be more efficient for length diameter ratio range of 100–500 and Reynolds number 40–1400 [4]. To abstain from the pressure losses nanofluids are administered as convective medium. Particle size, volume fraction and aspect ratio are the principal properties on which heat transfer is pivoted on [5]. Nanofluids have been subjected to extensive research to achieve the maximal convective heat transfer. The thermophysical properties of nanofluids are independent of temperature [6]. Nanofluids with smaller particles are found to have higher viscosity and Nusselt number for constant Reynolds number. An upswing of 32% heat transfer is accomplished in case of 1.8 vol%  $\text{Al}_2\text{O}_3$  nanofluid [7–9]. Integrated performance of Brownian motion and thermophoresis of nanoparticles elevates the turbulence and improve the energy bearing capacity leading to thermal instability [10]. In spite of its added resource requirements forced convection is more advantageous than the natural convection. Forced convection on heated surface with porous structures increases the convection [11]. The flow of the convective medium

\* Corresponding author. Tel.: +91 44 2220 3262.

E-mail addresses: [kalai@annauniv.edu](mailto:kalai@annauniv.edu) (S. Kalaiselvam), [guganms@yahoo.co.in](mailto:guganms@yahoo.co.in) (M.S. Gugan), [kuralau1252@yahoo.co.in](mailto:kuralau1252@yahoo.co.in) (E. Kuraloviyar), [mega619@gmail.com](mailto:mega619@gmail.com) (R. Meganathan), [anpriyan@gmail.com](mailto:anpriyan@gmail.com) (A. Niruthiya Priyan), [swami774@annauniv.edu](mailto:swami774@annauniv.edu) (M.R. Swaminathan).

### Nomenclature

$h$	convective heat transfer coefficient $W/m^2 K$
$T$	temperature K
$A$	area $m^2$
$W$	weight g
$M_s$	molecular weight g/mol
$C_c$	molar concentration mol/L
$V$	volume of the solvent L

### Subscripts

$t$	test plate
$b$	referral plate
$m$	bulk mean

can be disrupted by the porous structures in nanometric scale to achieve turbulence expeditiously. The size of the nanostructures plays an imperative role in initiating the flow turbulence. Nanoporous surface with smaller pore size will result in elevated capillary action [12]. By utilizing the nanoporous surface heat transfer rate can be proliferated 132% higher than the polished surface of bare metals. Fabrication of nanoporous layers can be done by assorted methods like electrochemical anodization, spray pyrolysis, plasma arc injection, chemical vapor deposition, ion beam etching, atomic force deposition and nanoparticle etching [13–15]. The nanoporous layer fabrication by electrochemical anodization and spray pyrolysis can be justified economically for implementing in industries [16,17]. This research work is contemplated to scrutinize the proliferation of heat transfer rate accomplished by nanoporous layers fabricated on the surface of the thermal conductors like copper, brass, and aluminium [18]. The design optimization is achieved for maximal heat transfer by analyzing the control parameters of nanoporous fabrication methods.

## 2. Methodology

The heat transfer characteristics are analyzed in three disparate modes. Polished bare metal plates with surface roughness  $0.2 \mu m$ , plates with nanoporous surface of pore size  $120 nm$  formed by electrochemical anodization, plates with nanoporous surface of pore size  $60 nm$  formed by spray pyrolysis. The attributes of the nanoporous test metal plates copper (C 12800), brass (C 23000), and aluminium (A 96063) are judged with stainless steel (S 30300) plate as reference and water as convective medium. Surface area of the test plates and the referral plate are maintained constant to have same heat flux. Temperature of test plate and referral plate is perpetuated at preset values by a microcontroller. In the experimentation it is assumed that the heat lost in test plate is equal to the heat gained in the reference plate. The fluid region inside the enclosure is considered adiabatic, because of homogenous thermal mixing of convective medium. To ascertain the convective heat transfer rate bulk temperature of convective medium is measured. The ratio of the heat loss of top plate  $h_t$  to loss of bottom plate  $h_b$  is enumerated to obtain the convective heat transfer rate of the test metal plate. The thermal balance between the top and bottom plates is expressed in equation (1).

$$h_t/h_b = (T_m - T_b)/(T_t - T_m). \quad (A_t = A_b) \quad (1)$$

where  $T_t$  is the temperature of the test plate,  $T_b$  is the temperature of the referral plate,  $T_m$  is the mean bulk temperature of water in the enclosure,  $A_t$  and  $A_b$  are the heat transfer area of the test plate and the referral plate respectively. The obtained ratio is considered as a new quantitative index for the heat transfer enhancement.

Electrochemical anodization process is a top down approach to yield nanoporous surface. In this process metal particles are removed in nanometric scale to make the surface porous. The test metal plate acts as anode and stainless steel plate is cathode. Both the plates are immersed in an electrolyte solution of  $1 M H_2SO_4$ .

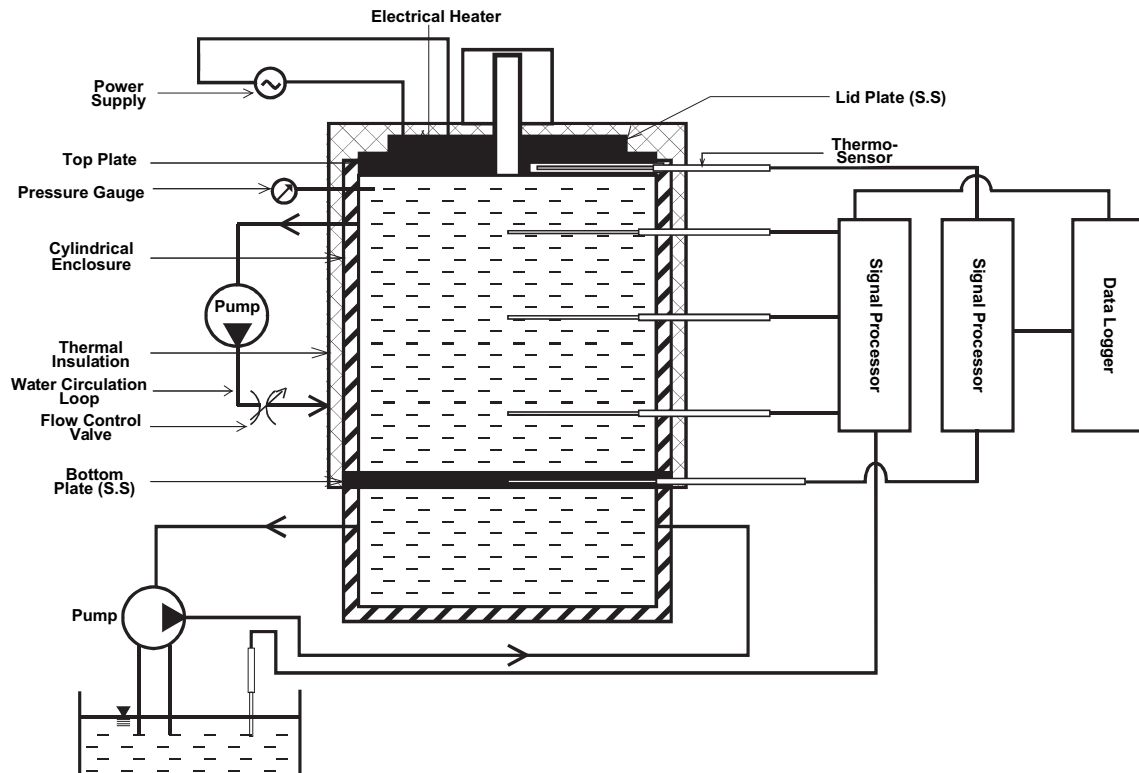


Fig. 1. Schematic of experimental set up.

A regulated power supply is employed to cater the oxidation potential of 1.4 V, 2–2.6 V, 2.5–3 V to the electrodes aluminum, brass, and copper respectively. Oxidation potential is incremented in steps of 0.1 V. The process is carried out for various machining time by replacing the test plates at time intervals of 30 s, 60 s and 120 s. The time for which the oxidation potential is supplied and the concentration of the electrolyte are the two important control parameters with which the pore size varies.

Spray pyrolysis is a bottom up approach to fabricate a surface with nanoporous structures. The precursor solution is pulverized as a fine mist with a 600  $\mu\text{m}$  spray nozzle and a carrier gas at high pressure of 50 bar. The mist condenses on the substrate forming a nanoporous layer on the substrate surface. The substrate must be assayed for acidity. The precursor solution is obtained by the controlled hydrolysis of copper acetate in distilled water. The precursor solution consists of fine dispersion of solid particles which range from 1 nm to 1  $\mu\text{m}$  in the liquid where the Brownian motions suspend the particles. The solution was stirred at room temperature for 2 days by a magnetic stirrer to yield a clear and homogeneous solution. The solution was then age hardened in the centrifugal type age hardener at room temperature. The precursor solution must be sprayed rhythmically over the ensconced substrate at operating temperature. The control parameters are concentration of precursor solution, viscosity of precursor solution, operating temperature, spray gun size, pressure of carrier gas, spray time, carrier gas. The temperature of the substrate plays an important role in the formation of porous layer, and is controlled by modifying the burner and sensed by an iron-constantan thermocouple touching the surface of the hot plate. The temperature of the metal surface is maintained below the recrystallisation temperature of the metal typically around 100  $^{\circ}\text{C}$ –500  $^{\circ}\text{C}$  so that there is no modification in the grain structure and grain boundaries of the substrate metal, which affect the heat transfer characteristics of the metal. Viscosity of the precursor solution can be enhanced by polymer admixtures like polyvinylpyrrolidene. The precursor solution should be sprayed at regular time intervals for the formation of nanoporous structure. Irregularity results in thin film formation. Concentration of the precursor solution can be determined using the equation (2).

$$W = \frac{M_s * C_c * V}{1000} \quad (2)$$

Where  $W$  is the weight of parent metal salt to be dissolved,  $M_s$  is the molecular weight of metal salt,  $C_c$  is the molar concentration, and  $V$  is the volume of the solvent.

### 3. Experimental setup and test procedure

The experimental setup shown in Fig. 1 incorporates enclosures for circulation of convective medium, measuring unit and control unit. Outer shell of the cylindrical encapsulation is made of Pyrex Borosilicate glass. Glass provides viable visibility while conducting the experiment. The test plate is placed at the top side of the enclosure. The stainless steel plate is secured at the bottom of the enclosure with slender sealants. A 110 W electrical heater is placed on the test plate and is controlled by a microcontroller. A well secluded cooling loop is positioned below the stainless steel plate. RTD sensors of accuracy  $\pm 0.1$   $^{\circ}\text{C}$  with a range of 0–760  $^{\circ}\text{C}$  and J Type thermocouples of accuracy  $\pm 0.1$   $^{\circ}\text{C}$  are employed to quantify the temperature in the system. PT 100 RTD's are positioned with congruent intervals along the centerline of the enclosure and are fenced of finely. Iron and constantan J type thermocouples are placed in 7 locations on the heater surface and the reference plate to measure the uniformity of the temperature. The sensors are connected to a data acquisition system to reckon the reliable heat transfer rate at regular recesses.

Pumps with flow control valve are used to bring off perennial flow of convective medium. Pressure rise inside the enclosure is gauged by a pressure sensor, of range 1–1000 bar and 0.1% FS accuracy over  $-10$  to  $+80$   $^{\circ}\text{C}$ , positioned at the vicinity of flow inlet and is linked to flow controller. The temperature of heater and cooler are retained at 50  $^{\circ}\text{C}$  and 20  $^{\circ}\text{C}$  respectively. The apparatus is shielded with thermal insulator of conductivity 0.018 W/mK. The water loops conducts itself as a convective medium. Heat transfer rate is computed for a perceptible increment in the temperature of convective medium with the data logger.

The convective heat transfer rate is obtained by the ratio of the heat loss of top plate  $h_t$  to that of bottom plate  $h_b$  and is represented in equation (1). The bulk mean temperature of the convective medium is measured by RTD sensors of accuracy  $\pm 0.1$   $^{\circ}\text{C}$  and the temperatures of test and referral plates are measured by J Type thermocouples of accuracy  $\pm 0.1$   $^{\circ}\text{C}$ . So that the estimated uncertainty in the heat loss ratio are about 5.9% at the lowest side and 5.04% at the highest one. The experimental uncertainty in the heat flux is, mainly due to experimental errors in the heat balance, the contact resistance between the plate heater and the test section plate surface, axial thermal conduction in the test plate section, the temperature measurements and the calculation of the heat transfer surface temperature. It was estimated to be  $\pm 7.45\%$ .

### 4. Results and discussion

Experimental results indubitably illustrate the influence of porous surface on heat transfer. The heat transfer ratio acquired for

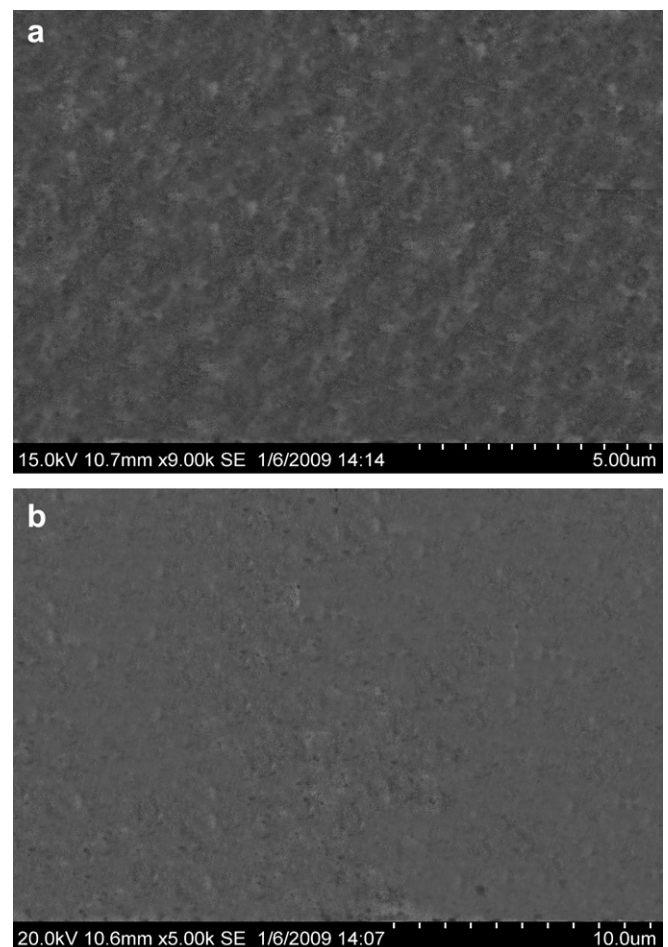


Fig. 2. a. SEM image of polished brass surface. b. SEM image of polished copper surface.

the polished metal surface with surface roughness  $0.2\ \mu\text{m}$  is 0.335 for copper, 0.32 for aluminium and 0.324 for brass. Polished copper exhibits higher heat rate than brass and aluminium, since the heat loss is proportional to the thermal conductivity. The SEM images shown in Fig. 2a and b reveal the surface of the polished metal surface of brass and copper with minimal waviness which provides insignificant impedance to the flow of convective medium.

The heat transfer rate is primarily pivoted on the surface attributes. The nanoporous surface proliferates the heat transfer rate predominantly. The irregularities at nanometric scale afford appreciable augmentation of convective heat transfer. Nanoporous surface with pore size 60–100 nm is formed by electrochemical anodization, which results in increase in surface area. The nanostructures scattered over the surface enhances the capillary action of convective medium. Hence more heat energy is transported by convection. The turbulence of the flow is achieved more expeditiously. Pore size plays a critical role, larger the pore size more will be the pressure rise in the system.

SEM images of the nanoporous surface formed in electrochemical anodization shown in Fig. 3a and b manifest the nanometric pores scattered over the surface of copper and brass. In copper and brass pores formed are uniform. In aluminium irregularities are formed as pores and cracks because of its semi crystalline nature and reactivity with the electrolyte. In electrochemical anodization the heat transfer rate for aluminium is 117%, brass is 127% and copper is 131% higher on comparison with the polished

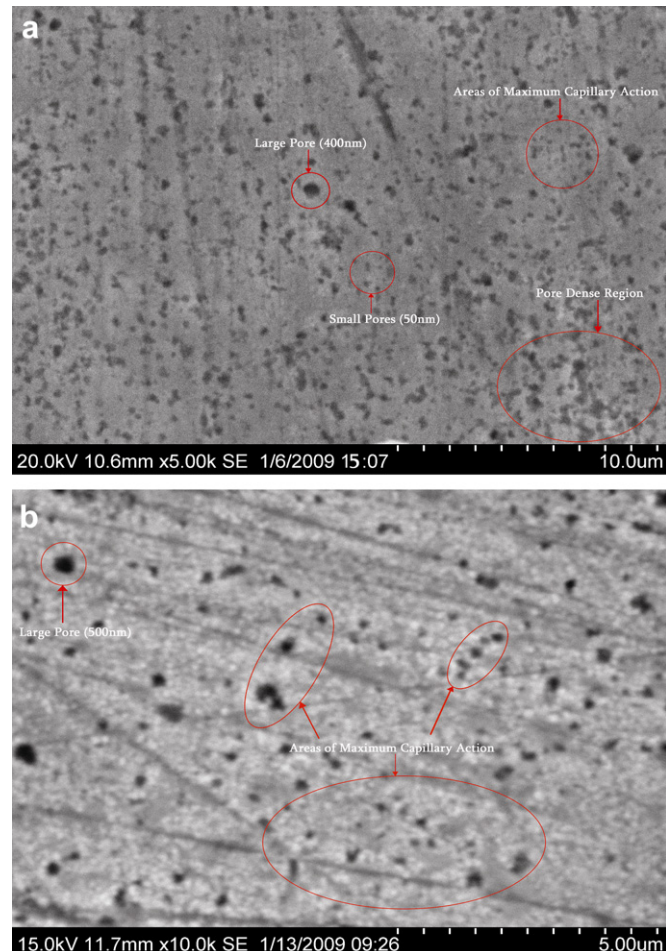


Fig. 3. a. SEM image of anodized nanoporous copper. b. SEM image of anodized nanoporous brass.

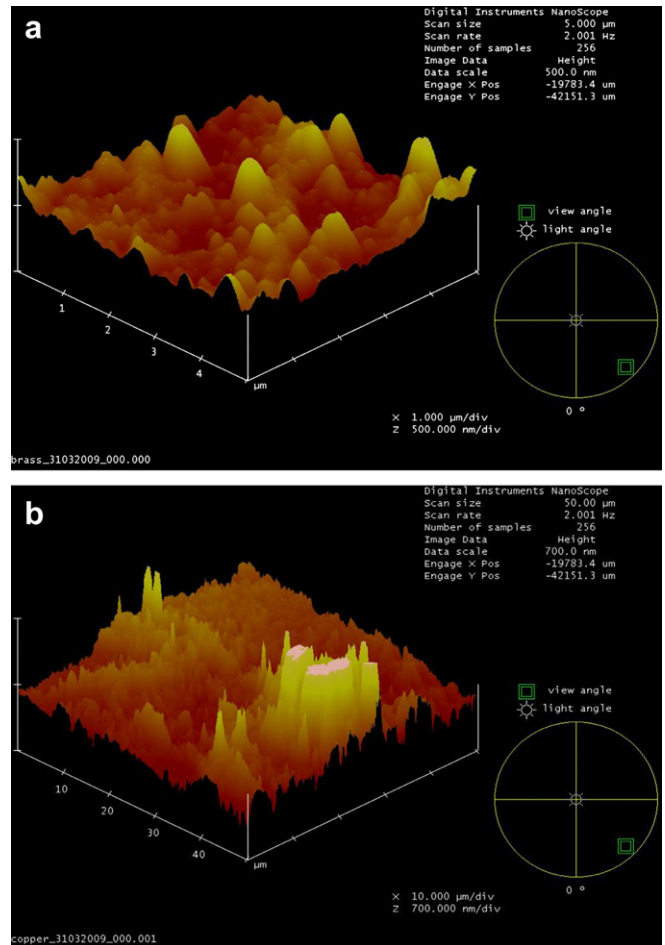


Fig. 4. a. AFM analysis of nanoporous brass. b. AFM analysis of nanoporous copper.

bare metals. The heat transfer ratio for the nanoporous surface with pore size 60–100 nm is 0.764 for copper, 0.705 for aluminium and 0.746 for brass.

The pore density, pore distribution and surface profile are analyzed with the atomic force microscopy (AFM). AFM images portray the productivity of the fabrication processes in forming a predictable nanoporous surface. AFM images shown in Fig. 4a and b picture the surface of brass and copper where the pores are distributed uniformly. The topography of the nanoporous surface is plotted in Fig. 5. The pores are deeper in case of aluminium because of its reactivity as presented in Fig. 6.

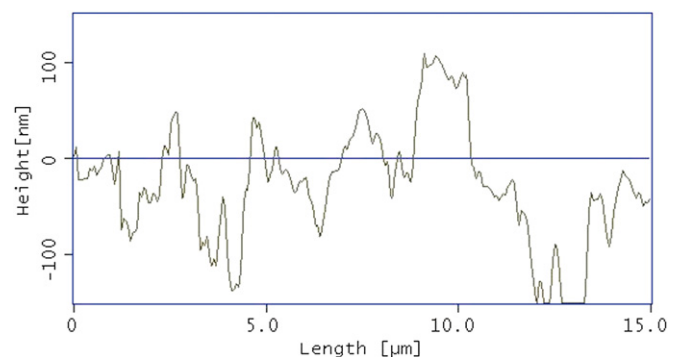


Fig. 5. Topography of nanoporous surface.

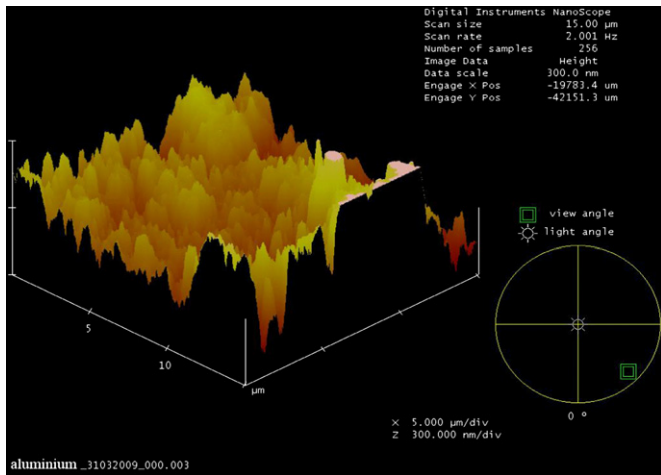


Fig. 6. AFM analysis of nanoporous aluminium.

SEM images of nanoporous layer fabricated in spray pyrolysis shown in Fig. 7a and b display the nanometric structures engineered on the copper and brass surface. The pores and cracks disrupt the flow and intensifies the convective heat transfer. The surface consists of unvaried nanopores of size 100–120 nm. The pore size can be governed by manipulating operating pressure, operating temperature, concentration and viscosity of precursor solution. In spray pyrolysis the heat transfer rate for aluminium is

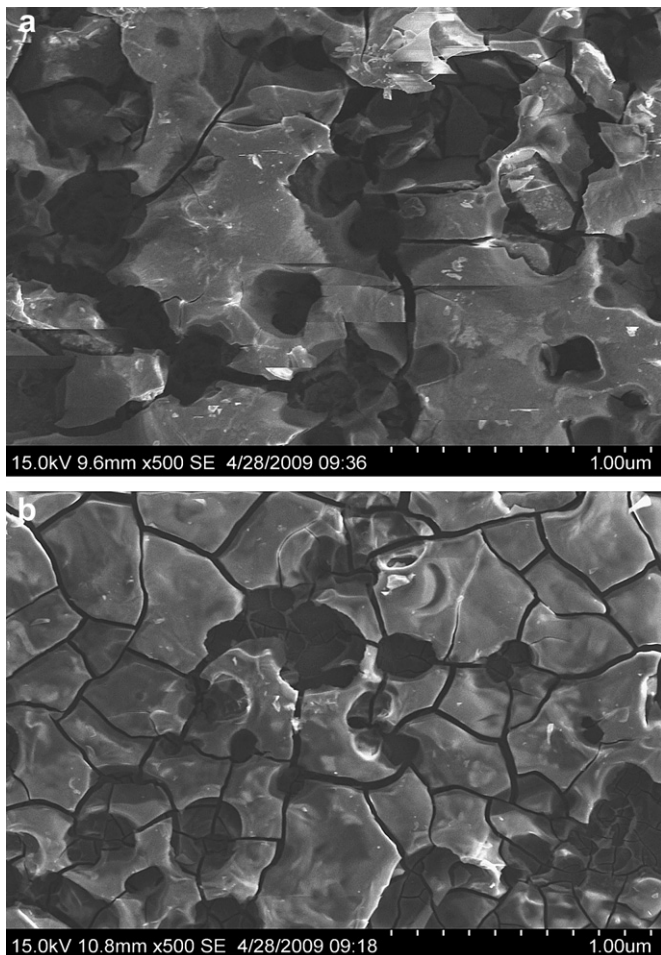


Fig. 7. a. SEM image of spray pyrolysed copper. b. SEM image of spray pyrolysed brass.

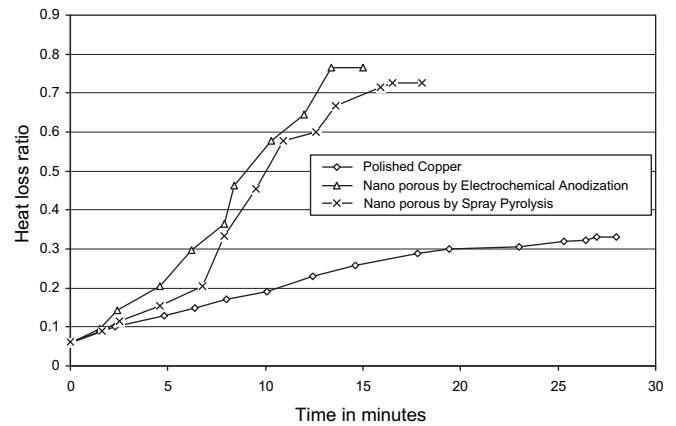


Fig. 8. Heat loss ratio comparison for copper.

109%, brass is 118%, and copper is 120% higher than the polished bare metals. The heat transfer ratio for the nanoporous surface with pore size 60–100 nm is 0.727 for copper, 0.681 for aluminium and 0.712 for brass.

The diversification of the heat loss ratio with time is computed for all the test plates and is represented in Figs. 8 and 9 which imply the influence of porosity on heat transfer for copper and brass. In case of nanoporous copper the maximum heat transfer is accomplished expeditiously. The maximum heat transfer is accomplished 200% faster in nanoporous copper than the polished bare metal. The graph presented in Fig. 10 indicates the effect of porous structures on heat transfer for aluminium. The swiftness with which the maximum heat transfer achieved is comparatively lesser in case of brass and aluminium. Electrochemical anodization is more efficient than the spray pyrolysis. This occurs because of the oxide film formed on the metal surface in spray pyrolysis. Precipitous proliferation of heat transfer rate is observed in nanoporous surface because of the capillary action and turbulence of the flow.

The effect of increase in heat transfer showed a distinct dependence on surface roughness. Fig. 11 illustrates the relation between the convective heat transfer coefficient ratio and the area ratio. It is renowned from the figure that area increase is having a positive effect on heat transfer coefficient to a certain limit after which, as the pore area increases, the diameter of the pore increases resulting in decrease in capillary effect thus decreasing the heat transfer coefficient. The turbulent comportment of the fluid on the nanoporous surface contributes to the enhanced heat transfer. Electrochemical anodization is thrifter than spray

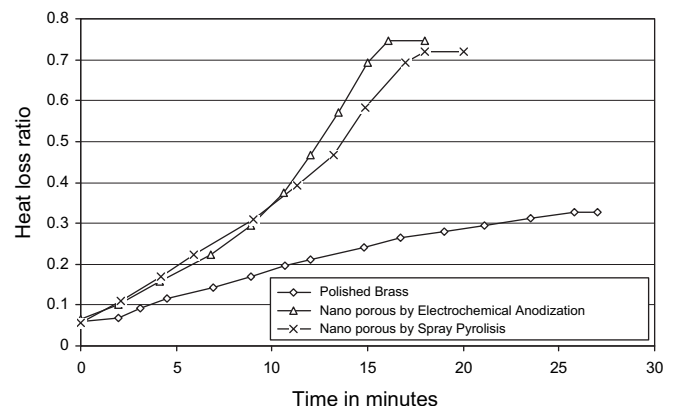


Fig. 9. Comparison of heat loss ratio for brass.

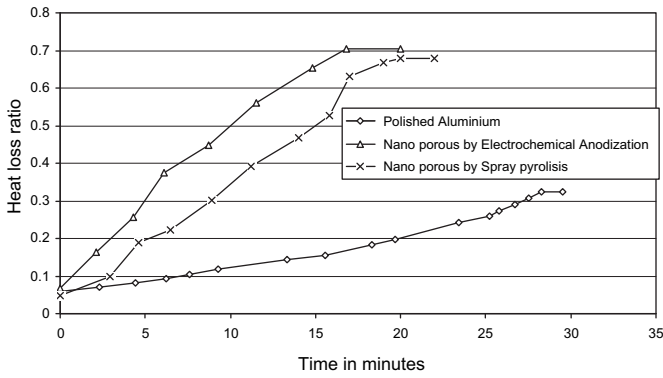


Fig. 10. Heat loss ratio comparison for aluminium.

pyrolysis because of the oxide formation and occurrence of shallow nanopores in the layer. In electrochemical anodization the change in surface area of the anodized metal with increase in reaction time is depicted in Fig. 12. In this process the material removal increases with reaction time. Between 120 s and 180 s material removal is uniform all over the surface. Hence the increase in surface area is high in this range. After 180 s shallow pores are formed with higher radius. Thus the increase in surface area is relatively less. In copper

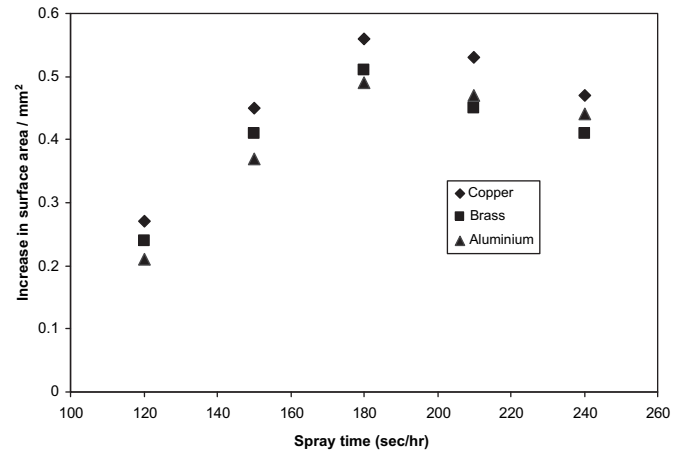


Fig. 13. Change in surface area with an increase in spray time.

increase in surface area is relatively high because of its electrochemical nature and high conductivity. The electrical conductivity of aluminium is about 60% that of copper per area of cross-section. In case of aluminium material removal rate is high, which leads to formation of shallow pores. In case of spray pyrolysis sol gel sprayed over the surface forms the nano porous layers. For a small spray time, the holes formed are also smaller, which is inferred in Fig. 13. At a spray time of 3 s/min, the increase in surface is high. When the spray time is more than 3 s/min, shallow holes are formed and overlapping of pores occurs, thus the increase in surface area is comparatively low. Increase in surface area on brass and aluminium is lower than copper because of the oxide formation on the surface at higher spray temperatures. In brass presence of zinc enhances the reactivity resulting in the formation of thin oxide layers.

The heat transfer between the substrate and the convective medium greatly depends on the nanoporous structures which have an effect on the static configuration and dynamic behavior of the convective medium in the vicinity of the surface. The convective medium form a sticky layer on the substrate surface periodically and statically, thus enabling a large amount of heat transfer in nanoporous structures. For copper heat transfer enhancement of 131% and 120% is achieved in case of electrochemical anodization and spray pyrolysis respectively. Electrochemical anodization and spray pyrolysis are more provident than other nanoporous fabrication methods like chemical vapor deposition, atomic force dispersion, plasma arc machining, and ion injection. Electrochemical anodization process can be used to form a nanoporous surface in complicated shapes but it involves electrode design. Spray pyrolysis is limited to small substrates.

5. Conclusion

Heat transfer rate has been evaluated for various bare metals and nanoporous surfaces in order to marvel at the magnification of convective heat transfer in nanoporous surface. This research concludes,

1. The nanoporous surface enhances convective heat energy transfer extensively. By fluctuating the pore size heat transfer rate can be varied.
2. Copper nanoporous surface accomplishes high convective heat transfer augmentation of 131% followed by brass and aluminium.
3. Optimization of pore size and operating pressure yields very high heat transfer augmentation.

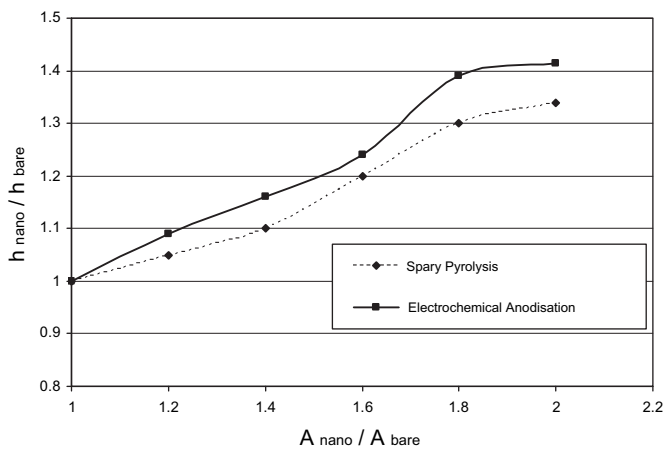


Fig. 11. Effect of nanoporous surface area on heat transfer.

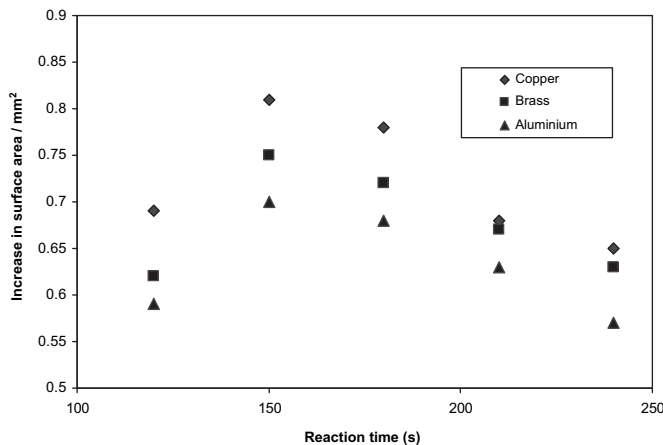


Fig. 12. Change in surface area for an increase in anodization time.

The propounded procedure of administering nanoporous surface to augment convective heat transfer can be utilized in refrigeration systems, heat exchangers, power plants and high heat energy transfer applications. The maximum heat transfer enhancement achieved in nanoporous surface of aluminum is 117%, brass is 127%, and copper is 131% higher than polished surfaces. Nanoporous surfaces prove to be an efficient method to enhance convection than the nanofluid system and active augmentation techniques.

### Acknowledgement

The authors gratefully acknowledge Dr. D. Arivuoli, Department of Physics, and Dr. S. Nanjundan, Department of Chemistry, Dr. S. Jeyavel, Centre for Nano technology, Dr. Kumar, Crystal growth centre, and Dr. K. Krishnamurthy, AUKBC Centre, Anna University Chennai for their constant support regarding nanoporous fabrication techniques and DST – FIST for providing the facilities available to perform this study. Finally we also thank Dr. B. Viswanathan, Department of Chemistry, IIT Madras, for his tireless support to perform this research.

### References

- [1] H. Gul, D. Evin., Heat transfer enhancement in circular tubes using helical swirl generator insert at the entrance. *International Journal of Thermal Sciences* 46 (12) (2007) 1297–1303.
- [2] A.G. Kanaris, A.A. Mouza, S.V. Paras, Optimal design of a plate heat exchanger with undulated surfaces. *International Journal of Thermal Sciences* 48 (6) (2009) 1184–1195.
- [3] Andrew. J.L. Foong, N. Ramesh, Tilak T. Chandratilleke, Laminar convective heat transfer in a microchannel with internal longitudinal fins. *International Journal of Thermal Sciences* 48 (10) (2009) 1908–1913.
- [4] O.N. Sara, O. Barlay Ergu, M.E. Arzutug, S. Yapöcö, Experimental study of laminar forced convective mass transfer and pressure drop in microtubes. *International Journal of Thermal Sciences* (2009). doi:10.1016/j.ijthermalsci.2009.01.021.
- [5] B.H. Chang, A.F. Mills, E. Hernandez, Natural convection of microparticle suspensions in thin enclosures. *International Journal of Heat and Mass Transfer* 51 (5–6) (2008) 1332–1341.
- [6] Sadik Kakac, Anchasa Pramuanjaroenkij, Review of convective heat transfer enhancement with nanofluids. *International Journal of Heat and Mass Transfer* 52 (13–14) (2009) 3187–3196.
- [7] Praveen K Namburu., Debendra K Das., Krishna M Tanguturi, Ravikanth S Vajjha, Numerical study of turbulent flow and heat transfer characteristics of nanofluids considering variable properties. *International Journal of Thermal Sciences* 48 (2) (2009) 290–302.
- [8] Jung-Yeul Jung, Hoo-Suk Oh, Ho-Young Kwak, Forced convective heat transfer of nanofluids in microchannels. *International Journal of Heat and Mass Transfer* 52 (1–2) (2009) 466–472.
- [9] K.B. Anoop, T. Sundararajan, Sarit K Das, Effect of particle size on the convective heat transfer in nanofluid in the developing region. *International Journal of Heat and Mass Transfer* 52 (9–10) (2009) 2189–2195.
- [10] D.Y. Tzou, Thermal instability of nanofluids in natural convection. *International Journal of Heat and Mass Transfer* 51 (11–12) (2008) 2967–2979.
- [11] Marie-Francoise Scibilia, Heat transfer in a forced Wall Jet on a heated rough surface. *Journal of Thermal Science* 9 (1) (2000) 85–92.
- [12] Peixue Jiang, Zhan Wang, Zepei Ren, Buxuan Wang, Forced convective heat transfer in a porous plate channel. *Journal of Thermal Science* 6 (3) (1997) 197–206.
- [13] O. Näth, A. Stephen, J. Rösler, F. Vollertsen, Structuring of nanoporous nickel-based superalloy membranes via laseretching. *Journal of Materials Processing Technology* 209 (10) (2009) 4739–4743.
- [14] A. Dallanora, T.L. Marcondes, G.G. Bermudez, P.F.P. Fichtner, C. Trautmann, M. Toulemonde, R.M. Papaléo, Nanoporous SiO<sub>2</sub>/Si thin layers produced by ion track etching: dependence on the ion energy and criterion for etchability. *Journal of Applied Physics* 104 (2008) 024307/1–024307/8.
- [15] L. Menon, K. Bhargava Ram, S. Patibandla, D. Aurongzeb, M. Holtz, J. Yun, V. Kuryatkov, K. Zhub, Plasma etching transfer of a nanoporous pattern on a generic substrate. *Journal of the Electrochemical Society* 151 (7) (2004) 492–494.
- [16] Dainius Perednis, Ludwig J Gauckler., Thin film deposition using spray pyrolysis. *Journal of Electroceramics* 14 (2005) 103–111.
- [17] D. Todorovskya, R. Todorovska, N. Petrova, M. Uzunova-Bujnova, M. Milanova, S. Anastasova, E. Kashchieva, S. Groudeva-Zotova, Spray-pyrolysis, deep- and spin-coating deposition of thin films and their characterization. *Journal of the University of Chemical Technology and Metallurgy* 41 (1) (2006) 93–96.
- [18] W.F. Gale, T.C. Totemeier, *Smithells Metals Reference Book*, eighth ed. Elsevier, 2004.